

**GLOBAL JOURNAL OF ADVANCED ENGINEERING TECHNOLOGIES AND SCIENCES****DEVELOPMENT AND CALIBRATION OF REDUCED-ORDER BUILDING ENERGY MODELS BY COUPLING WITH HIGH-ORDER SIMULATIONS****Rongpeng Zhang\*, Omer T. Karaguzel**\* School of Architecture, Carnegie Mellon University, Pittsburgh, PA 15213, USA  
Well Living Lab, Rochester, MN 55902, USA

DOI: 10.5281/zenodo.3689397

**ABSTRACT**

Building energy modeling and simulation is an effective approach to evaluate building performance and energy system operations to achieve higher building energy efficiency. The high-order building models can offer exceptional simulation capacity and accuracy, however, its high level of complexity does not allow it to directly work with the optimization algorithms and methods that require a complete differential-algebraic-equations-based mathematical description of the physical model. In order to fill in the gap, the study presents a systematic approach to develop and calibrate the reduced-order building models. A notable feature of the approach is its coupling with high-order building simulations in order to pre-process the input information and support the calibration of the reduced model. A case study on a representative office building shows that the developed reduced-order model can present acceptable simulation accuracy compared with high-order simulations and significantly reduce the modeling complexity.

**KEYWORDS:** Reduced-order, building model, high-order simulation, model calibration.**INTRODUCTION**

The building sector has become the largest portion of energy end use in the world, exceeding both the industry and the transportation sectors. According to the US Department of Energy and the European Parliament and Council, buildings, both commercial and residential, account for about 40% of the total energy consumption in US and Europe [1, 2]. In order to achieve higher building energy efficiency, engineers and scientists have paid extensive attention to understand the performance of the building energy systems through simulation-based quantitative assessments.

The building energy systems consist of several major elements that are related to the building thermal performance, including the Heating Ventilation and Air Conditioning (HVAC) system, internal heat/moisture sources (electric lighting, occupants, etc), thermal masses (building envelope, furniture, etc) and the outdoor and indoor environments. The hygrothermal responses of a building can be considered as the consequences of the dynamic interactions between these elements. In addition, these elements are directly or indirectly related and interacted. For example, the changes of outdoor climatic conditions can affect both the operational efficiency and capacity of the HVAC system and the hygrothermal behavior of the building enclosures, which further influence the indoor thermal conditions [3-5].

The underlying basic physical phenomena in the building energy system include the conductive, convective and radiative heat transfer as well as the dependent moisture migration and buffering, which follow the fundamental heat and mass transfer principles. Although the basic transport theory has been well developed, it is quite challenging to build a mathematical building energy system model that is completely based on the first principles, due to the complexity and diversity intrinsic to buildings. In the previous research, many scholars developed first-principle based single-zone building models for different research purposes. It is reasonable and may be necessary to implement such lumped building models, especially when the study purpose is to deeply investigate selective building components/features [3, 6-11] or to investigate the application of new control/optimization methods for various building energy systems [12-17]. However, it usually requires tremendous manual work to apply the developed model for other building spaces with different geometrical characteristics and thermal response properties, and therefore, it may not be widely applied in realistic building analysis.

In a different vein, the techniques of whole building energy simulation and building information modeling have obtained significant progress in the past two decades, with the help of great advances in the computational power

and algorithms. These techniques have a much stronger capability in handling the building energy modeling challenges mentioned above. Several mature advanced building simulation engines have been developed by different institutions in the past two decades, such as DOE-2 [18], BLAST [19], EnergyPlus [20, 21], TRNSYS [22] and DeST [23]. They have been widely used throughout the world to support the building physics research and the actual new construction or retrofitting building design, operation and management. Although these engines may implement different modeling methodologies and/or program structures and thus have different advantages and features, they all share the following common capabilities: 1) to handle the high-order building energy models containing the detailed information about the functional and physical characteristics of the buildings 2) to perform co-simulation of a large number of subroutines to obtain more accurate estimations on the heat and mass energy flows throughout buildings [20].

Among these simulation engines, EnergyPlus, developed by LBNL Simulation Research Group and U.S. DOE, is a state-of-art and the most widely recognized simulation engine in the building energy efficiency field. It is a collection of many program modules that can work simultaneously, allowing the real-time interaction among different model components [20, 21]. It has been well tested and validated via a number of research projects and has been applied in a wide variety of building design and evaluation cases [24-31].

The high-order building energy engine has many great features in terms of simulation capacity and accuracy, however, it can only be treated as a black-box when cooperating with other control or optimization programs due to its high level of complexity [32, 33]. It cannot directly work with the algorithms and methods that require a reduced-order model that includes a complete DAE based mathematical description of the physical model. Therefore, how to develop reduced-order models that can provide DAE descriptions while offering more accuracy and flexibility than the first-principle based lumped models is a problem to be solved. This study aims to fill in the gap by presenting a systematic approach to develop and calibrate the reduced-order building model. The developed reduced building model consists of several sub-models for various load components, which are simulated simultaneously to determine the building transient sensible and latent cooling load. The approach couples with high-order building simulations to pre-process the input information for the reduced model and support the calibration of the reduced model.

### FRAMEWORK OF THE REDUCED-ORDER MODEL DEVELOPMENT

This study proposes an approach to develop reduced building energy models by coupling with the high-order building energy simulations conducted within EnergyPlus. It aims to generate DAE descriptions of the building models by making full use of the high-order building simulation features. The general idea is to extract from EnergyPlus program the modules that are directly related with the optimization tasks and transfer them into corresponding reduced-order models as described in the following sections of the study. The other modules are operated by EnergyPlus engine to calculate the parameters that are not directly correlated with the control variables in the system operation, for example, the solar incident radiation and zone infiltration airflow rate. Such parameters are treated as the inputs to the reduced models.

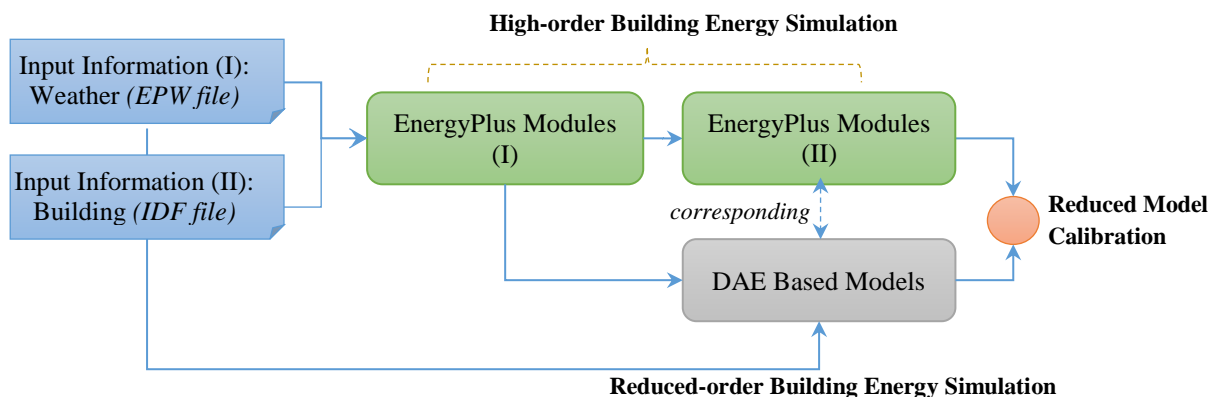


Fig. 1 Flow diagram of reduced-order model development

The framework of the reduced-order model development procedure is depicted in Fig. 1. As can be seen in the diagram, the high-order building energy simulation performs as two roles in the framework:

- EnergyPlus Modules (I): pre-process the input information for the reduced model, including the IDF file containing a complete building model description and the EPW file containing the typical meteorological year (TMY) weather data to construct external environmental conditions for a specific location;
- EnergyPlus Modules (II): support the calibration of the DAE-based reduced models.

The proposed procedure can bring several significant advantages for the reduced model development:

- A big portion of simulation task is shared by well-tested high-order building models, for example, the analysis of the shading effect between different buildings or components. Compared with the method incorporating all the modules in the reduced model, this tends to increase the simulation reliability and accuracy.
- After the high-order model pre-processing the weather and building information, the reduced-order model only need to deal with a considerable reduced amount of input information. This makes it much less challenging and time consuming to develop the reduced building model.
- The procedure has the capability to analyze realistic buildings with many thermal zones (i.e., HVAC blocks) and complex geometric configurations. Moreover, the developed reduced model can be slightly modified to apply to other buildings with different physical and functional characteristics.
- Having the high-order simulation as a bridge, the proposed reduced building model has the potential to cooperate with a large variety of commercial building modeling software existing in the current Architecture Engineering & Construction (AEC) industry.

The reduced building model is built in the MATLAB computing environment which is well recognized for its powerful programming and visualization functions [34]. The interconnection between the EnergyPlus and MATLAB simulations is achieved via MLE+, an open-source co-simulation platform developed by University of Pennsylvania [35]. It makes use of the advanced Energy Management System (EMS) feature within EnergyPlus to allow the couple of different simulation programs for distributed simulation or real-time simulation related to the building energy system [36, 37].

### MODEL REDUCTION FOR THE COOLING LOAD COMPONENTS

Three substantial time delay effects intrinsic in the building heat and moisture transfer have to be well addressed in the reduced building model development, including:

- Radiant time delay effect: delay of radiative heat gain conversion to building cooling loads
- Conduction time delay effect: delay of conductive heat gain through external building envelopes
- Time delay effect due to the thermal storage and moisture buffering of internal thermal mass

In the high-order building simulations, the sub-models addressing the first two effects are too complex to be described by DAEs, and therefore, the corresponding reduced order models are derived and then calibrated by high-order building thermal simulations. The third delay effect can be addressed by DAE based model.

### RADIANT TIME SERIES (RTS) BASED REDUCED MODEL FOR RADIATION COOLING LOAD EVALUATION

The radiative heat gains must first be absorbed by the interior room surfaces, and then be converted to the cooling load when it is later transferred by convection from those surfaces to the room air. Thus, a surface by surface heat balance analysis is necessary to perform the first-principle based radiative cooling load estimation. However, it is usually very challenging and time-consuming to include the first-principle based radiative cooling load estimation in a DAE based model.

In the study, the reduced model handling the radiation cooling load calculations is derived from the Radiant Time Series Method (RTSM) which is originally developed in the late 1990s [38-40]. Compared with the heat balanced method (HBM) implemented in the high-order building simulations, RTSM is a transformation-based procedure that can be described by DAEs in a simpler form, requiring a much less amount of input information. Such characteristics make it well-suited for the reduced-order model development in the study.

RTSM was first developed to perform peak design cooling load calculations for the purpose of HVAC system sizing. Instead of solving the instantaneous convective and radiative heat transfer from surface by surface analysis, it provides a simplified transformation-based approach to quantify the radiative heat gain conversion to cooling loads.

The key concept of the method is radiant time series (RTS), which are used to address the time-dependent response of the zone to the radiant energy pulses. RTS contains a group of radiant time factors specifying the portion of the radiant pulse that is convected to zone air in the current and the following hours. In other words, these factors reflect the distribution of radiant heat gains over time. When estimating the cooling load for a specific hour, radiant time factors are multiplied with the corresponding radiant heat gains occurred in both the current and past hours [38, 40].

Most heat gains sources within buildings (such as through lights, people, walls, roofs, windows, internal equipment) transfer energy by both convection and radiation. RTSM applies an estimated coefficient to split each of the heat gain components into convective and radiation portions. The convective portion is treated as instantaneous cooling load, and the radiation portion is treated using radiant time factors corresponding to the heat gain types. Thus, the cooling load contributed by a single load component for a specific hour is the sum of the instantaneous convection portion from that component and the time-delayed portion of radiant heat gains.

In the reduced model development for radiation cooling load evaluation, the concept of RTS is implemented while the specific procedures are further improved. With the support of EnergyPlus simulations, several features of traditional RTSM are expanded as summarized below:

- Traditional RTSM computes building loads for a 24-hour design day based on the assumption of steady-periodic conditions, that is, the weather conditions and the building operations of the design day are identical to those of previous days. In the proposed procedure, however, this assumption is not necessary because EnergyPlus can be used to provide the necessary information of previous days. Therefore, it is able to perform cooling load calculations for a much longer period, rather than peak load estimation for only the design day.
- Theoretically, a separate series of radiant time factors is needed for each unique zone, since different massiveness and arrangement of zone construction surfaces may lead to diverse thermal response characteristics. In the traditional RTSM, this cannot be achieved because the users are only allowed to determine a specific set of RTS from pre-tabulated factors. During this process, designers need to use their experience to select the zone types that most closely match the actual situation, but this may not be clear in all cases [41]. In the proposed procedure, however, the RTS for each zone can be derived separately by the optimization algorithms during the calibration process. This tends to create a higher degree of accuracy than the traditional RTSM.

Fig. 2 shows the detailed steps for developing the RTS based reduced models for radiation cooling load evaluation. Firstly, EnergyPlus is activated to perform the pre-processing of the input building and weather information and perform calculations of the heat gains for each radiation-related load component, such as the transmitted solar heat gains for each window and the internal lighting heat gains. Secondly, the calculated heat gains are imported to the reduced model for further analysis. In the reduced model, the convective/radiative split coefficient is applied to separate the radiation and convection portion for the heat gains, and the radiant time factors are applied to process the radiative heat gains of different types. Thirdly, the instantaneous convective heat gains and the processed radiative heat gains are added together to obtain the cooling load profiles for these radiation-related load components.

In the study, three series of radiant time factors are implemented for different radiation types:

- Direct solar RTS: for analyzing the directly transmitted solar radiation
- Diffuse solar RTS: for analyzing diffuse solar radiation
- Internal radiation RTS: for analyzing the radiant heat gains from internal heat sources, including occupants, lights and equipment.

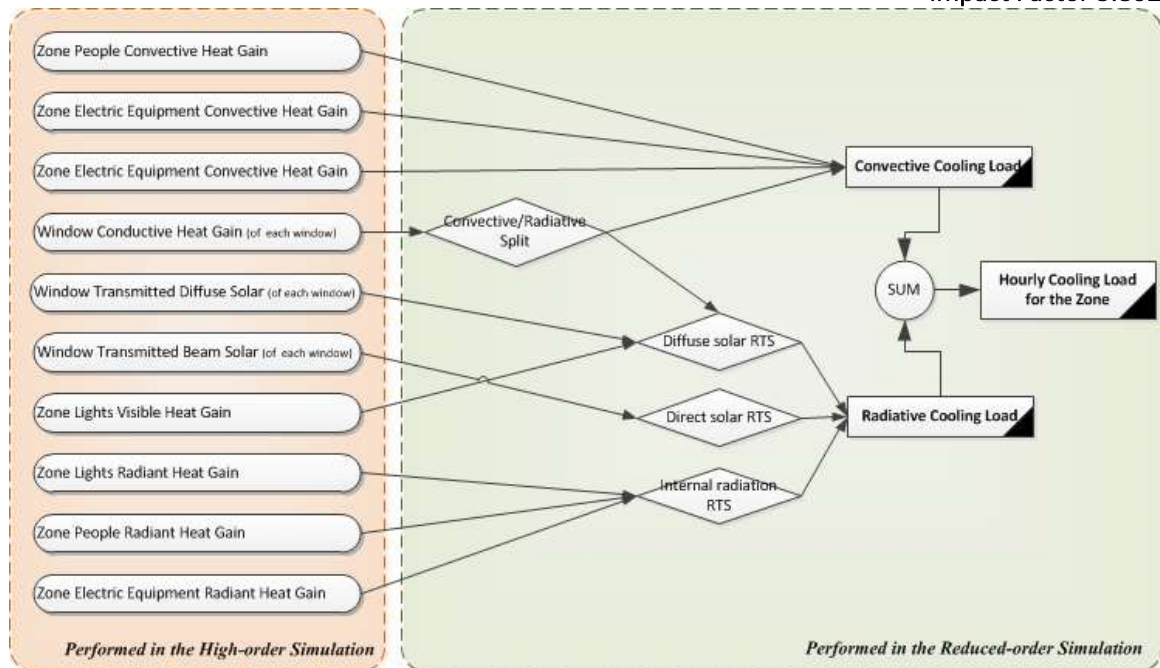
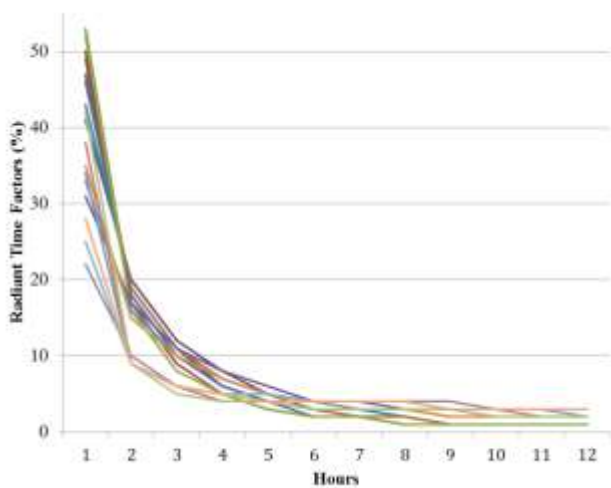
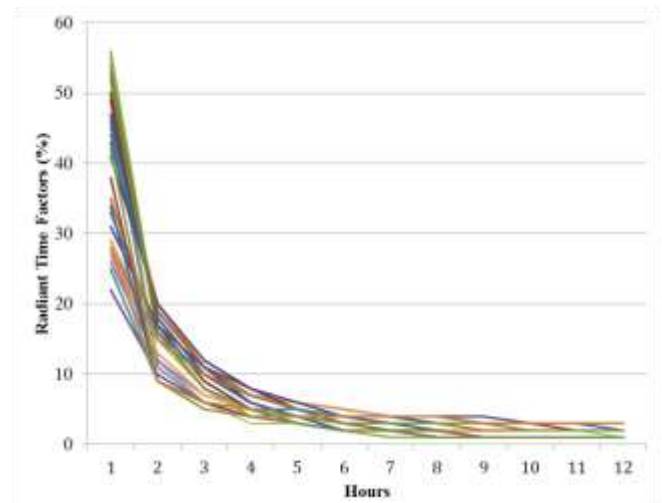


Fig.2 Overview of the procedure for RTS based reduced model for radiation cooling load evaluation

Fig. 3 illustrates the RTS values for a group of representative constructions [40]. These typical RTS values set up a range which will be used as the feasible region in determining the RTS for a specific zone during the calibration process (refer to section 2.4 for more details on the reduced model calibration).



(l) RTS for solar radiation



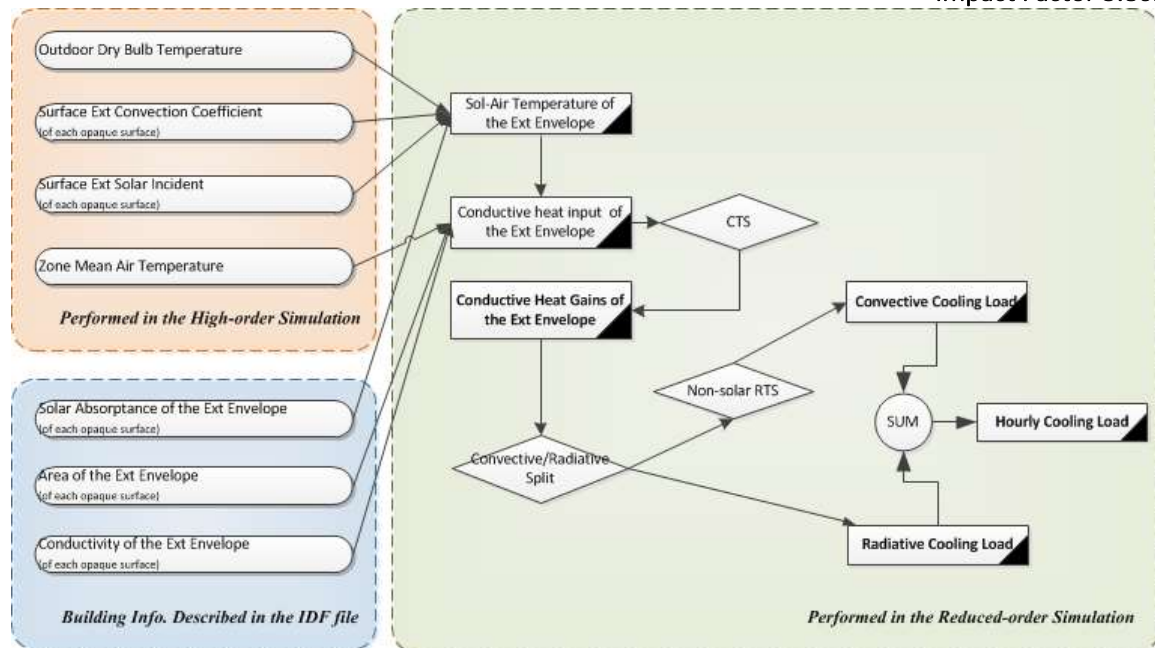
(r) RTS for non-solar radiation

Fig.3 RTS values corresponding to a group of representative constructions

**CONDUCTION TIME SERIES (CTS) BASED REDUCED MODEL FOR CONDUCTIVE COOLING LOAD EVALUATION**

Conduction time series (CTS) are used here to develop the reduced model to address the time delay effect of conductive heat gain through external building envelopes. Similar to the RTS described above, CTS uses a group of conduction time factors to specify the portion of the conductive heat input at the exterior envelope that is converted to the zone conductive heat gains in the current and the following hours.





**Fig.4 Overview of the procedure for developing the CTS based reduced model for conductive cooling load evaluation through external envelopes**

Fig. 4 shows the detailed steps to perform CTS based conductive cooling load evaluations. Firstly, the sol-air temperatures for each external surface are calculated as

$$T_{sol-air} = T_0 + \frac{\alpha E_t}{h_0} - \frac{\varepsilon \Delta R}{h_0} \tag{1}$$

where

- $E_t$  total solar radiation incident on the external surface [W/m<sup>2</sup>·K]
- $h_0$  convection heat transfer coefficient at the external surface [W/m<sup>2</sup>·K]
- $T_0$  outdoor air temperature [K]
- $\alpha$  solar absorptance of the external surface [--]
- $\varepsilon$  hemispherical emittance of the external surface [--]
- $\Delta R$  difference between long-wave radiation incident from sky/surroundings on the surface and the radiation emitted by blackbody at outdoor air temperature; can be ignored for most vertical surfaces [W/m<sup>2</sup>]

Secondly, the conductive heat input for each surface is calculated using the sol-air temperatures calculated above:

$$q_c = UA(T_{sol-air} - T_i) \tag{2}$$

where

- $A$  area of the surface [m<sup>2</sup>]
- $T_i$  indoor air temperature [K]
- $T_{sol-air}$  sol-air temperature for the external surface [K]
- $q_c$  conductive heat input of the external surface [W]
- $U$  overall heat transfer coefficient for the surface [W/m<sup>2</sup>·K]

After that, the conductive heat gains of the surface for a specific hour can be obtained by multiplying the conduction time factors with the corresponding conductive heat inputs occurred in both the current and past hours:

$$Q_{c,\theta} = c_0 q_{c,\theta} + c_1 q_{c,\theta-1} + \dots + c_N q_{c,\theta-N} \tag{3}$$

where

- $c_0 \dots c_N$  conduction time factors for the surface [--]
- $N$  number of hours that the effect of a conductive heat input can last [h]
- $Q_{c,\theta}$  conductive heat gain of the zone for the current hour ( $\theta$ ) [W]
- $q_{c,\theta-n}$  conductive heat input of the external surface n hour ago [W]

Finally, the calculated conductive heat gains are split into convective and radiation portions and further handled with non-solar RTS as described in section above.

Fig. 5 illustrates CTS values for a group of representative constructions that are commonly used in the industry and summarized in the ASHRAE handbook [40]. During the calibration process, the CTS values for each wall are selected within the range formed by these typical CTS values.

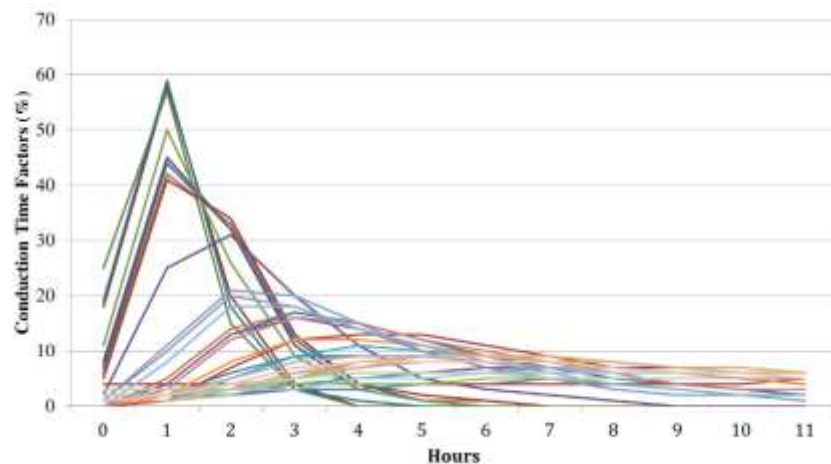


*Fig.5 CTS values corresponding to a group of representative constructions*

#### HEAT AND MOISTURE MIGRATION THROUGH EXTERNAL ENVELOPES

Compared with the convective moisture transfer via infiltration and ventilation, the amount of moisture transfer through external envelopes is usually of a much smaller magnitude and the corresponding latent heat gain is not significant. Therefore, the moisture diffusion via external envelope is often neglected in the indoor air humidity balance analysis [42, 43]. However, it is critical to take the moisture into account to study the sensible load through envelopes, since the moisture content within the envelope may present a considerable impact on the material thermal properties and thus change the heat transfer behaviors of the envelope [44].

In the study, the Combined Heat and Moisture Transfer (HAMT) model is implemented in the EnergyPlus simulations to address the coupled moisture and heat migrations in the envelope, and then the high-order simulation results are used to calibrate the conduction time series (CTS) based reduced model which only involves the heat transfer.

#### THERMAL STORAGE AND MOISTURE BUFFERING IN THE INTERNAL THERMAL MASS

Interior building materials may present a considerable time delay effect which tends to dampen the fluctuations of the indoor temperature and humidity fluctuations. Depending on the interior material characteristics, moisture absorption/desorption processes of interior building materials can remove/deliver different amounts of moisture to the indoor air environment. According to Diasty, indoor room surfaces can absorb as high as one third of the moisture generated in the room space [42].

The Effective Moisture Penetration Depth (EMPD) Model is implemented in the study to simulate the thermal storage and moisture buffering effect of the building materials. It is a lumped approach developed on the transient heat and mass transfer analogy. The model can simulate the heat storage and moisture buffering response for most building materials, especially when the material surface resistance is large compared to the internal resistance for moisture flow [45]. Note that the EMPD model is described by DAE equations with an acceptable level of complexity, and thus can be directly implemented in the reduced building model without the calibration procedure.

#### REDUCED BUILDING MODEL CALIBRATION BY INTEGRATED SIMULATION

In this section, the developed reduced model is calibrated using the EnergyPlus simulation results for a representative office building. A single-objective multivariable optimization problem is formulated in order to capture the proper settings of the reduced model.

### CONFIGURATIONS OF THE CASE BUILDING

The case building selected in this study is a medium-sized commercial office reference building provided by the U.S. Department of Energy Building Technologies Program [21]. It is a three story office building with a total conditioned floor area of 4982 m<sup>2</sup>. It has the same plan layout for each floor, as depicted in Fig. 6. The building definition is given in the form of whole-building energy simulation model compatible with EnergyPlus program [46]. It includes both perimeter and core zones and meets the minimum requirements for commercial buildings given by American Society of Heating Refrigeration and Air Conditioning Engineers (ASHRAE) 2010 Building Energy Standard 90.1 [47].

The model is simulated under the environmental boundary conditions for Chicago, IL, U.S. (41 °N, 87°W), which is classified as ASHRAE Climate Zone 5A and has a heating dominated, cool and humid weather conditions with annual heating and cooling degree days of 3430 and 506, respectively (18 °C baseline). Ideal loads air system intended for load calculations is implemented in the model, which exactly maintains the desired temperature setpoint of 25°C for cooling and 18°C for heating by varying the air flow rate.

The four perimeter zones in a typical middle floor are selected in the study. These zones have external walls facing to four orientations and thus represent four types of cooling load characteristics. More details on the building/zone configurations can be found in [48].

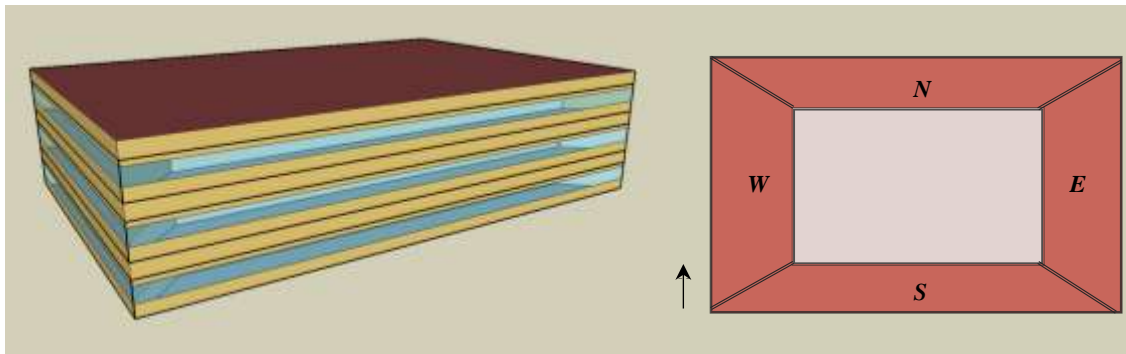


*Fig.6 Exterior view (l) and plan layout (r) of the case building*

### ENERGY AND MOISTURE BALANCES FOR THE BUILDING ZONE AIR

The zone air model is developed to predict the indoor temperature and humidity conditions, taking into account the dynamic interactions between indoor environment and other cooling load components such as building enclosure and occupants. The zone air model introduced in this section and the other sub-models developed in the previous sections form a whole building hygrothermal model for further optimization analysis.

The temperature condition for a specific zone is the consequence of the balance between heat gains and losses from the zone space. The heat fluxes incorporated in the zone air model include [21, 40]:

- (1) conductive cooling load of the zone through opaque external envelopes,
- (2) radiant cooling load of the zone through windows,
- (3) convective heat transfer with interior building materials,
- (4) heat transfer by ventilation,
- (5) heat transfer by mechanical air conditioning system,
- (6) heat transfer by infiltration,
- (7) cooling load due to internal operational activities.

Similarly, the humidity conditions for a specific zone is the consequence of a number of moisture fluxes [9, 21, 49], including:

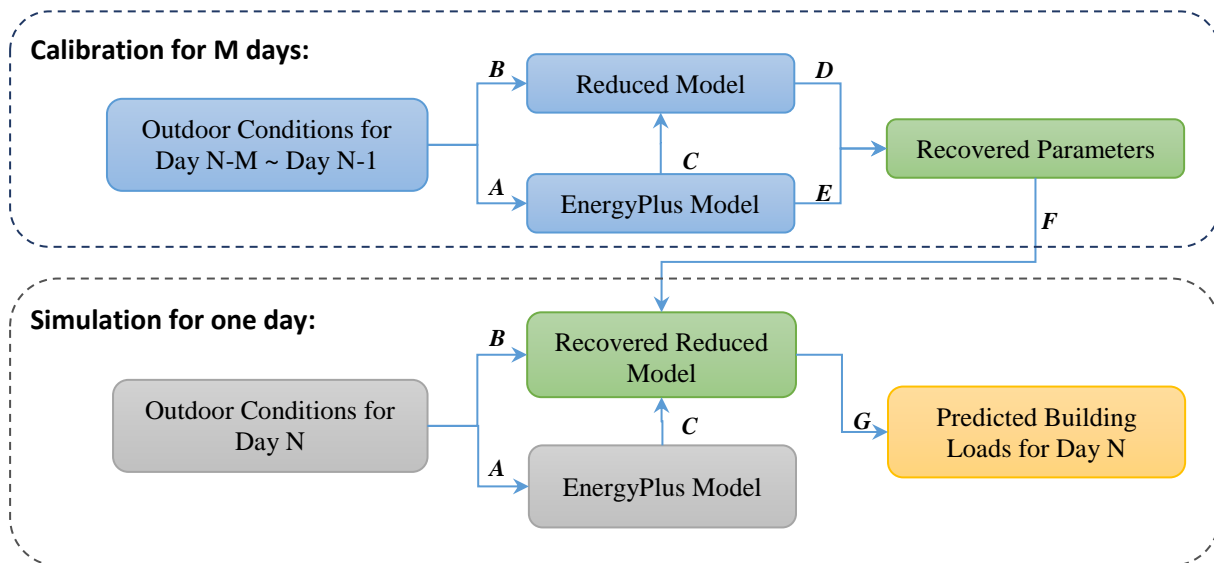
- (1) moisture absorption/desorption of interior hygrothermal building materials,
- (2) moisture supply and removal by ventilation,
- (3) moisture addition and removal by mechanical system,
- (4) moisture supply and removal by infiltration,
- (5) moisture addition into zone due to internal operational activities.



**PROCEDURE FOR THE REDUCED MODEL CALIBRATION AND SIMULATION**

Fig. 7 shows the specific calibration and simulation workflows for the reduced model development. It is carried out in the following two successive steps:

- (1) The calibration is performed for an M-day period (e.g., M is 3 in this case study) to recover the reduced model, by comparing the reduced model simulations with the EnergyPlus simulations;
- (2) The recovered reduced model performs the simulation for the following one day, and the calculated building cooling loads are compared with the EnergyPlus simulation results to evaluate the performance of the reduced model.



Note: Labels A-G are the parameters transferred between models/components (refer to [4] for details)

**Fig.7 Calibration and simulation procedure for the reduced model development**

**OPTIMIZATION FORMULATION FOR THE CALIBRATION**

The purpose of the calibration is to configure the reduced model such that it can perform building thermal performance evaluations as similarly to the high-order models as possible. More specifically, the difference between the building cooling load predictions by the reduced-order and high-order simulations should be minimized.

This can be taken as a single-objective multivariable optimization problem with the objective function defined by:

$$\min \sum_{i=1}^{N_s} \sum_{j=1}^{N_z} (Q_{h,i,j} - Q_{r,i,j})^2 \tag{4}$$

where

- $N_s$  number of time steps in the calibration period [--]
- $N_z$  number of building thermal zones [--]
- $Q_{h,i,j}$  cooling load at time step i for zone j by the EnergyPlus simulations [W]
- $Q_{r,i,j}$  cooling load at time step i for zone j by the reduced-order simulations [W]

In the study, the calibration is performed for a 3-day period with a 15-minute time interval, and thus the value of  $N_s$  is 288 (i.e., the division of the calibration period and the time).

The minimization is achieved by manipulating the variables describing the reduced model, including:

- Direct solar RTS (surface level)
- Diffuse solar RTS (surface level)
- Internal radiation RTS (thermal zone level)
- CTS values (surface level)
- Convective/radiation split coefficient (surface level)

As mentioned in section 2.3, a group of CTS and RTS values corresponding to a number of typical constructions are used to set the constraints for the optimization problem. The mean of these typical values is chosen as the initial value in the optimization.

The solution of the minimization is achieved in the MATLAB environment, using constrained nonlinear multivariable optimization method, namely *fmincon* [50]. In the study, it can solve the optimization for a single 3-day calibration with computation times of several CPU minutes.

**RESULTS AND DISCUSSIONS**

**Performance Evaluation of the Recovered Reduced Model**

The reduced model calibration and simulation is performed for the four study zones of the case building for July (96 time steps per day).

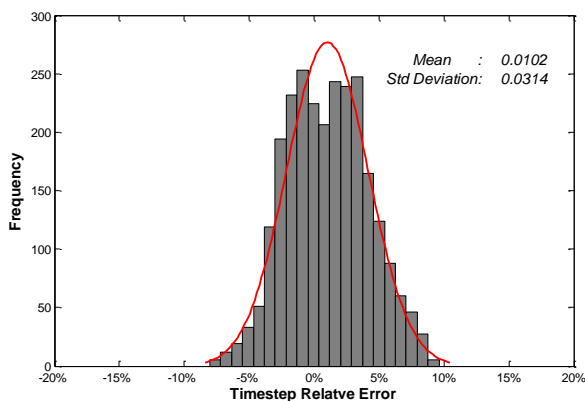
To quantitatively evaluate the performance of the recovered reduced model, the relative error (RE) for each time step is defined as:

$$RE_{i,j} = \frac{Q_{h,i,j} - Q_{r,i,j}}{Q_j} \times 100\% \tag{5}$$

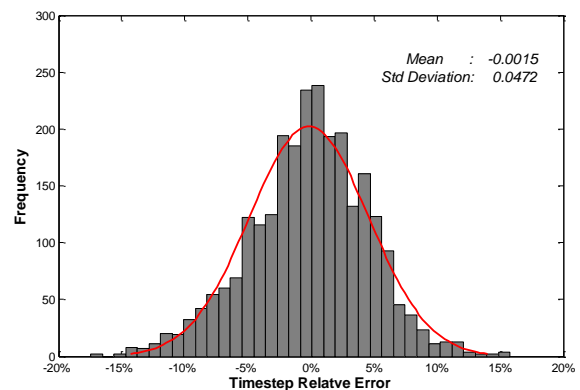
where

- $Q_{h,i,j}$  cooling load predictions at time *i* for zone *j* by EnergyPlus simulations [W]
- $Q_{r,i,j}$  cooling load predictions at time *i* for zone *j* by reduced-order simulations [W]
- $Q_j$  average cooling load during the office hours of the day for zone *j* [W]

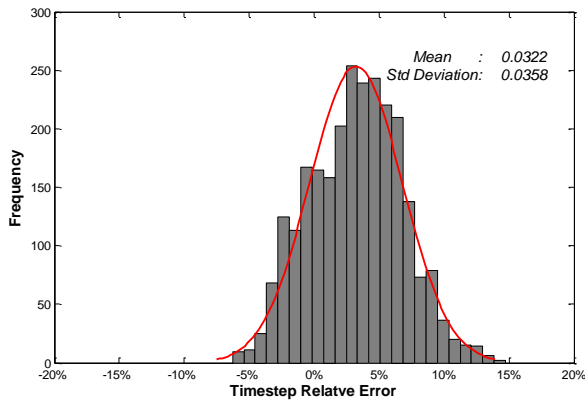
The RE distributions for each zone are depicted in Fig.8. Although the RE for different zones have slightly different distributions, they can generally be kept at low levels, mostly within  $\pm 10\%$ . The fitted normal distributions have the mean value between  $-0.15\% \sim 3.22\%$  and the standard deviation between  $3.14\% \sim 4.72\%$ . This means that the recovered reduced model can generate an acceptable level of simulation accuracy.



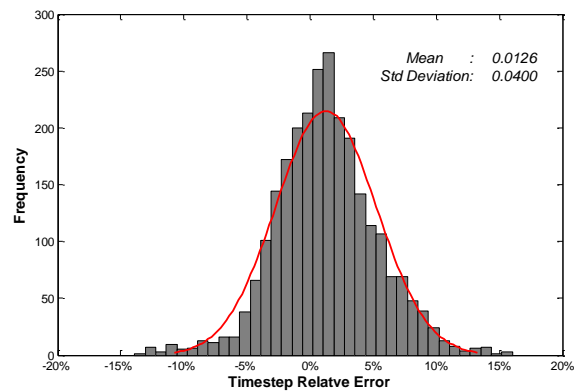
(a) South Zone



(b) East Zone

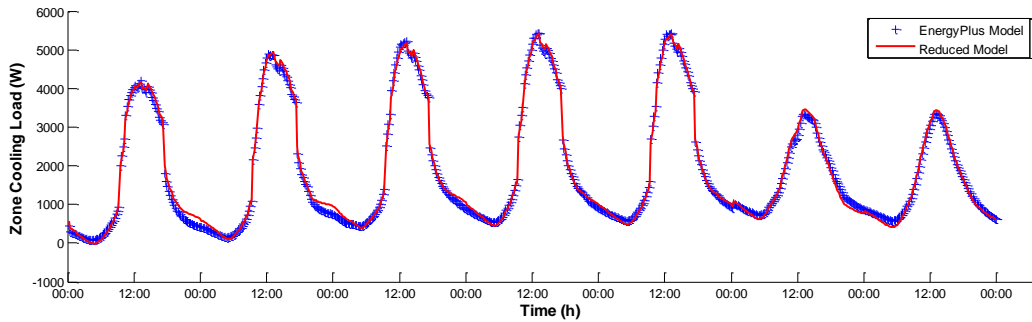


(c) North Zone

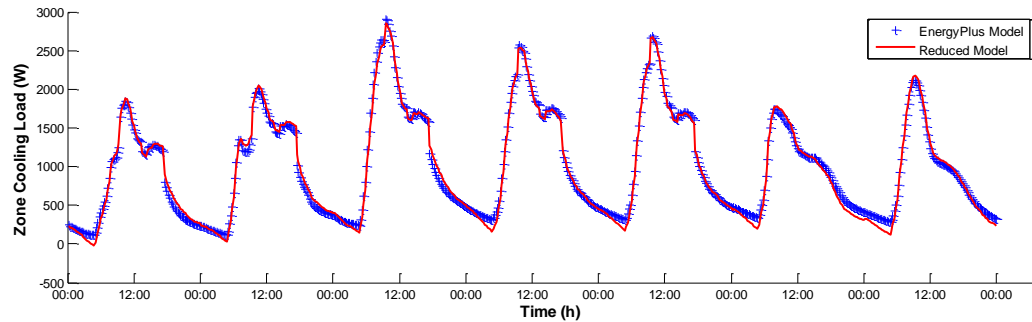


(d) West Zone

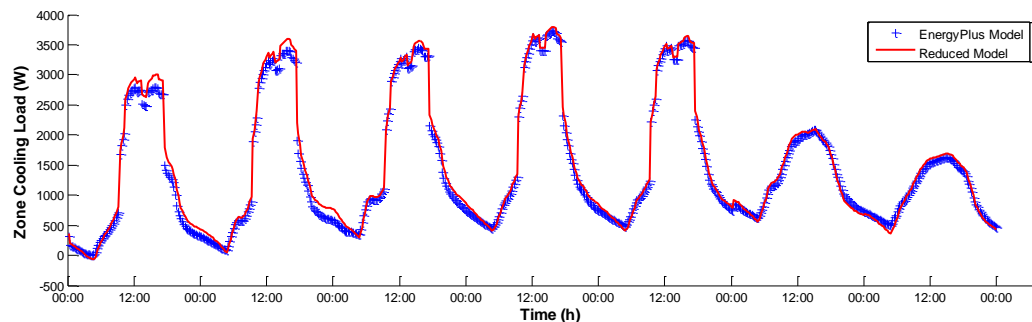
Fig.8 Relative error distribution of the reduced model simulations for one month (July)



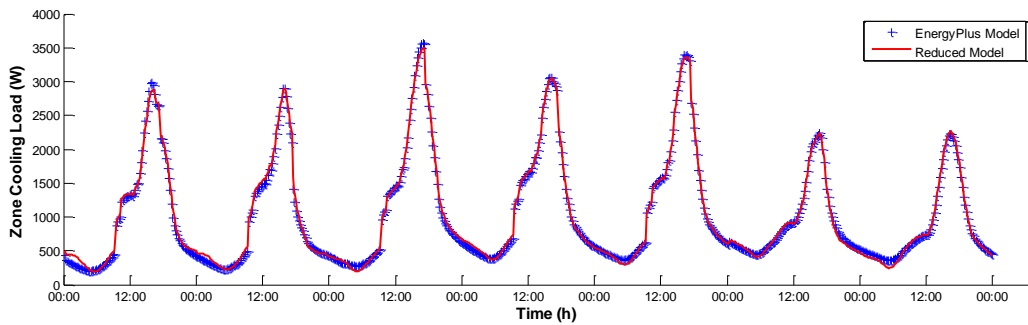
(a) South Zone



(b) East Zone



(c) North Zone



(d) West Zone  
(One typical week: Jul. 14-20)

**Fig. 9 Comparison of the cooling load predictions by the the EnergyPlus and reduced model simulation**

The cooling load predictions by the the EnergyPlus and the reduced model for a typical week (Jul. 14-20) is displayed in Fig. 9. It intuitively shows the agreement between the reduced model and high-order model simulations. It can be seen that both the weekdays (Jul. 14-18) and the weekends (Jul. 19-20) can be well simulated by the reduced model, although they have quite different operational schedules.

Note that the four zones present daily cooling load profiles with diverse patterns, as shown in Fig. 10. More specifically, the cooling load of the east zone achieves its peak at around 10:00am in the morning, while that of the west zone has a peak at around 4:00pm in the afternoon. The north and south zones present symmetric load profiles with the peaks at around 2:00pm. Such diversity mainly results from the zone orientation dependent solar radiation patterns, and may leads to remarkably influence on the operational strategy design for the air conditioning systems.

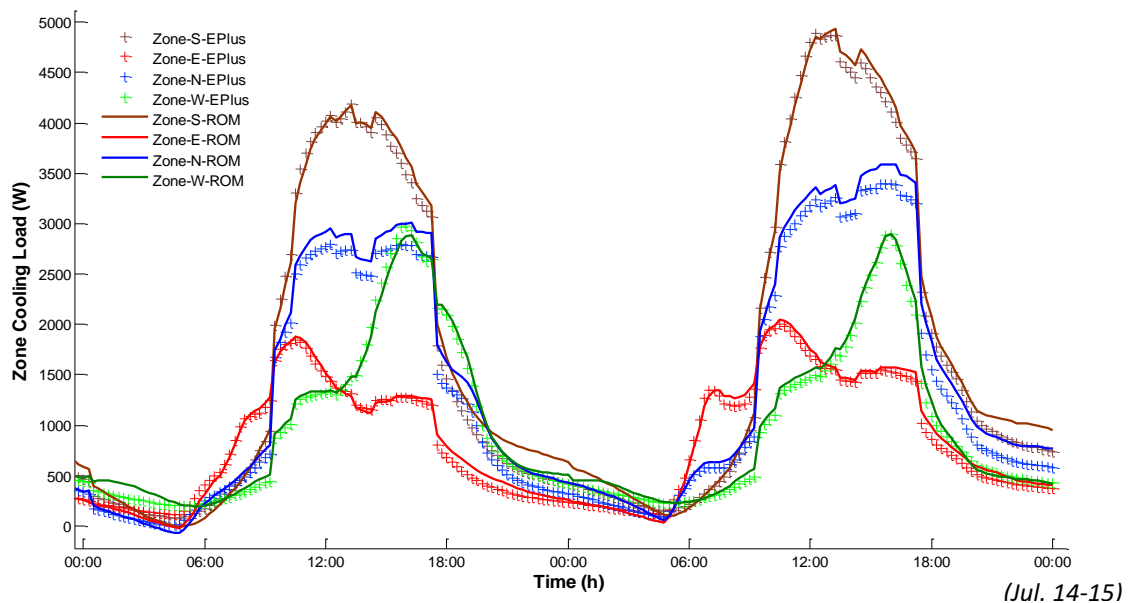
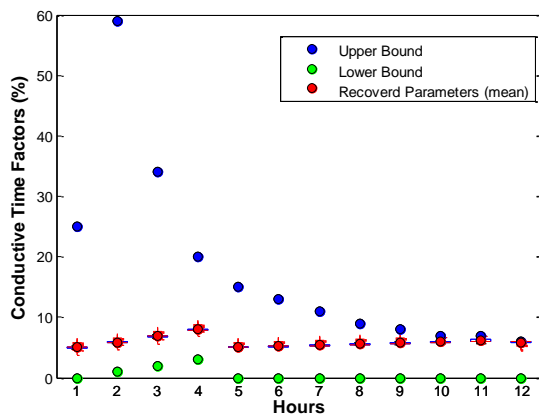
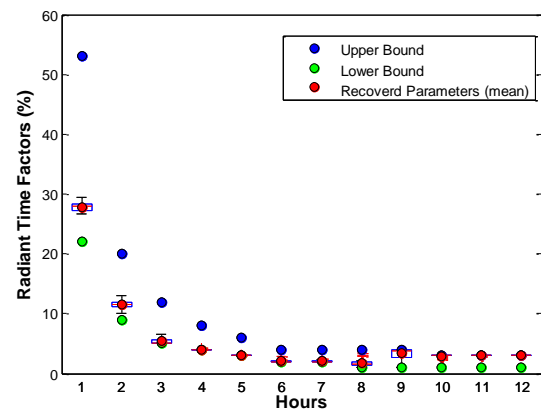


**Fig.10 Comparison of the daily cooling load profiles for four zones**

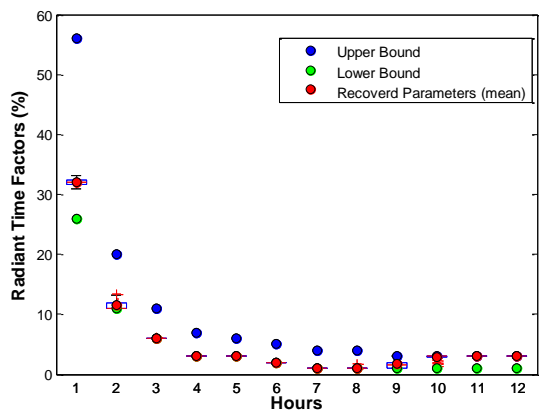
A set of CTS and RTS values is obtained for each 3-day calibration for each zone, so about 120 sets (product of the number of zones and the number of simulation days) are obtained in the monthly study of the four zones discussed above. It is found that the four zones have similar RTS and CTS profiles, which is largely due to the similar shapes and surface configurations of the different zones. Fig. 11 shows the distribution of the recovered CTS and RTS sets as well as the corresponding upper and lower bounds in the optimization. It can be seen that the recovered values tightly gather together with a small deviation.



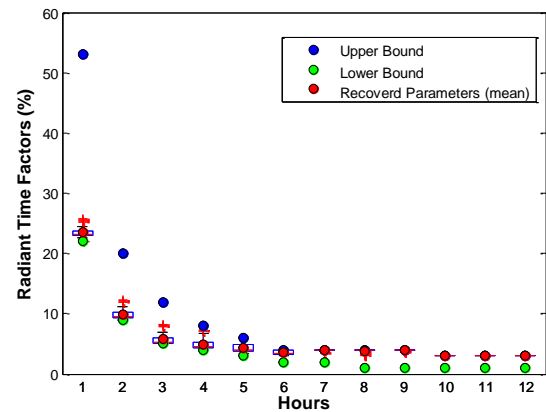
(a) External wall CTS



(b) Internal radiation RTS



(c) Direct solar RTS



(d) Diffuse solar RTS

Fig.11 Recovered CTS and RTS values in the calibration for one month (July)

In sum, the developed reduced-order building model can be well calibrated with the support of high-order EnergyPlus simulations following the proposed procedures. In the monthly study for the case building, the calibrated model can make satisfactory cooling load predictions for all the study zones for both the weekdays and weekends.

### PARAMETER SENSITIVITY ANALYSIS AND RANKING

As introduced above, there are 12 time factors in each of the RTS/CTS sets. In order to understand the importance of these time factors in the calibration, the QR factorizations with a column permutation (QRcp) method is applied in the reduced building model to perform parameter sensitivity analysis and ranking [51, 52].

QRcp method is an effective approach for parameter selection and estimation through successive orthogonalization of the sensitivity matrix derivative for parameter ranking. Based on orthogonal factorization, the method is easy to implement and the results are easily interpreted [51, 52].

The scaled sensitivity coefficient matrix used in the QRcp algorithm can be expressed as [52, 53]:



$$X = \begin{bmatrix} \left. \frac{\theta_1^*}{y^*} \frac{\partial y}{\partial \theta_1} \right|_{t_1} & \left. \frac{\theta_2^*}{y^*} \frac{\partial y}{\partial \theta_2} \right|_{t_1} & \dots & \left. \frac{\theta_{P-1}^*}{y^*} \frac{\partial y}{\partial \theta_{P-1}} \right|_{t_1} & \left. \frac{\theta_P^*}{y^*} \frac{\partial y}{\partial \theta_P} \right|_{t_1} \\ \left. \frac{\theta_1^*}{y^*} \frac{\partial y}{\partial \theta_1} \right|_{t_2} & \left. \frac{\theta_2^*}{y^*} \frac{\partial y}{\partial \theta_2} \right|_{t_2} & \dots & \left. \frac{\theta_{P-1}^*}{y^*} \frac{\partial y}{\partial \theta_{P-1}} \right|_{t_2} & \left. \frac{\theta_P^*}{y^*} \frac{\partial y}{\partial \theta_P} \right|_{t_2} \\ \vdots & \vdots & \ddots & \vdots & \vdots \\ \left. \frac{\theta_1^*}{y^*} \frac{\partial y}{\partial \theta_1} \right|_{t_{N-1}} & \left. \frac{\theta_2^*}{y^*} \frac{\partial y}{\partial \theta_2} \right|_{t_{N-1}} & \dots & \left. \frac{\theta_{P-1}^*}{y^*} \frac{\partial y}{\partial \theta_{P-1}} \right|_{t_{N-1}} & \left. \frac{\theta_P^*}{y^*} \frac{\partial y}{\partial \theta_P} \right|_{t_{N-1}} \\ \left. \frac{\theta_1^*}{y^*} \frac{\partial y}{\partial \theta_1} \right|_{t_N} & \left. \frac{\theta_2^*}{y^*} \frac{\partial y}{\partial \theta_2} \right|_{t_N} & \dots & \left. \frac{\theta_{P-1}^*}{y^*} \frac{\partial y}{\partial \theta_{P-1}} \right|_{t_N} & \left. \frac{\theta_P^*}{y^*} \frac{\partial y}{\partial \theta_P} \right|_{t_N} \end{bmatrix} \quad (6)$$

where

- $t_1, \dots, t_N$  the time-step points [--]
- $y$  responses, i.e., time-step cooling load [W]
- $y_i^*$  the cooling loads corresponding to the recovered RTS and CTS values [W]
- $\theta_1, \dots, \theta_P$  parameters to be estimated, i.e., RTS and CTS values [--]
- $\theta_i^*$  the recovered RTS and CTS values in the calibration [--]

The elements of the matrix, named individual parametric sensitivity coefficients, are numerically determined as described in [52].

Then the matrix singular value decomposition is carried out for X, as:

$$X = U D V^T \quad (7)$$

where D is a diagonal matrix of the same dimension as X, with nonnegative diagonal elements in decreasing order, and U and V are unitary matrices.

It is assumed that the estimated parameters are affected by noises following a Gaussian distribution with zero mean and covariance matrix  $\Sigma_\theta$ , which follows:

$$\Delta_\theta^T \Sigma_\theta^{-1} \Delta_\theta = \gamma \quad (8)$$

$\Sigma_\theta$  and X can be expressed by:

$$\begin{aligned} \Sigma_\theta &= (X^T \Sigma_y^{-1} X)^{-1} = (V D^T U^T \Sigma_y^{-1} U D V^T)^{-1} \\ &= \left( V D^T U^T \frac{I}{\sigma_y} U D V^T \right)^{-1} = \sigma_y (V D^T U^T U D V^T)^{-1} \\ &= \sigma_y (V D^T D V^T)^{-1} = \sigma_y (V \Lambda V^T)^{-1} \end{aligned} \quad (9)$$

where

- $\Sigma_\theta$  covariance matrix of the estimated parameters [--]
- $\Sigma_y, \sigma_y$  covariance matrix of the responses [--]

The triangular matrix  $\Lambda$  gives an easy form of the variance contribution of individual parameters, and is used as the criteria to assess the influence of the estimated parameters on the responses. The results for all the RTS/CTS sets are compared in Fig. 2.25.

It can be observed that in all the RTS/CTS sets, the first several time factors present more influence on the cooling load outputs of the reduced model, in other words, the first ones are more prominent in the calibration than the later ones. Therefore, it is reasonable to choose only the first time factors in the RTS/CTS sets in the calibration, such as the first 6, in order to balance the calibration accuracy and the computational complexity. This may be very critical in analyzing buildings with complex configurations, which usually present a large parameter set.

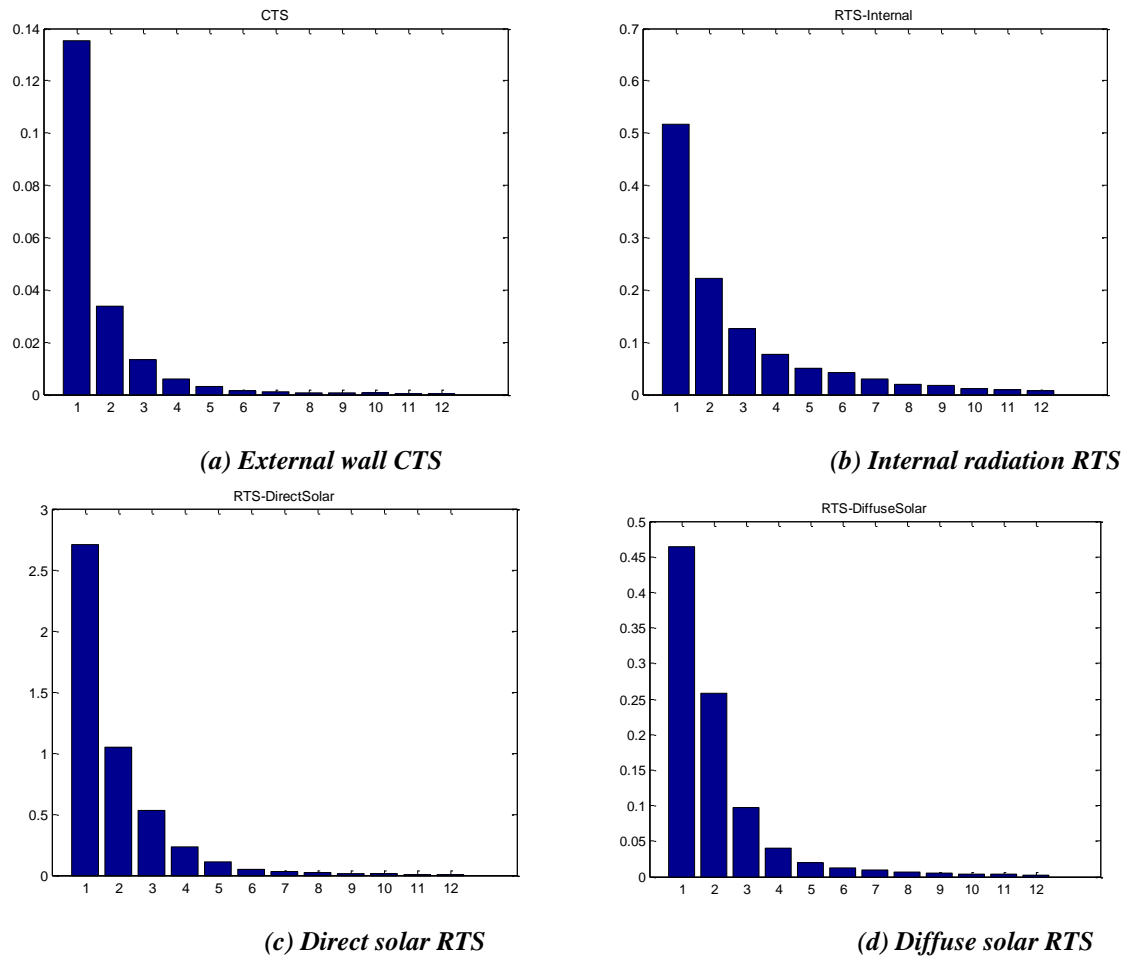


Fig. 12 Variance contribution of CTS and RTS values for parameter sensitivity analysis and ranking

## CONCLUSION

Building energy modeling and simulation is an effective approach to provide quantitative assessments of the building performance and energy system operations to achieve higher building energy efficiency. To overcome the limitations of existing high-order building models and first-principle based lumped models, the paper presents a systematic approach to develop and calibrate the reduced-order building model by coupling with high-order building simulations. The developed reduced-order model can offer a complete differential-algebraic-equations-based mathematical description of the physical model so that it can be directly implemented in some advanced building analysis such as system operation optimizations. Meanwhile, it offers higher simulation accuracy and flexibility than the first-principle based lumped models. The approach makes full use of the high-order building simulation features to support the reduce-order model, including pre-process the input information and support the calibration of the reduced model.

A case study was performed on a representative medium-sized commercial office building with four perimeter zones. These zones had external walls facing to four orientations and thus represent four types of cooling load characteristics. The results of calibration and simulation for a typical month showed an acceptable level of simulation accuracy for all the study zones. The fitted normal distributions of the relative errors had the mean value between -0.15%~3.22% and the standard deviation between 3.14%~4.72%. A QR factorizations with a column permutation method was applied in the reduced building model to perform parameter sensitivity analysis and ranking on the time factors in the RTS/CTS sets. Based on the analysis, suggestions were provided on reduced-order model development to balance the modeling accuracy and the computational complexity.

## REFERENCES

- [1] DOE, Buildings Energy Data Book. 2011, Office of energy efficiency and renewable energy, U.S. Department of Energy: Washington D.C.
- [2] EPC, Directive 2010/31/EU of the European Parliament and of the Council of 19 May 2010 on the energy performance of buildings. Official Journal of the European Union, 2010. L153: p. 13–35.
- [3] Tariku, F., K. Kumaran, and P. Fazio, Integrated analysis of whole building heat, air and moisture transfer. *International Journal of Heat and Mass Transfer*, 2010. 53(15–16): p. 3111-3120.
- [4] Zhang, R., Dynamic optimization based integrated operation strategy design for passive cooling ventilation and active building air conditioning. 2014, Carnegie Mellon University: Pittsburgh.
- [5] Zhang, R., Y. Nie, and K.P. Lam, Dynamic Optimization of the Integrated Operation Strategies for the Building VAV System and Night Ventilation using the Simultaneous Collocation Method: a Case Study, in *Proceedings of the Building Simulation and Optimization Conference (BSO12)*. 2012: Loughborough, UK. p. 237-244.
- [6] Yang, L. and Y. Li, Cooling load reduction by using thermal mass and night ventilation. *Energy and Buildings*, 2008. 40(11): p. 2052-2058.
- [7] Lapinskiene, V. and V. Martinaitis, The Framework of an Optimization Model for Building Envelope. *Procedia Engineering*, 2013. 57(0): p. 670-677.
- [8] Qin, M., et al., Simulation of coupled heat and moisture transfer in air-conditioned buildings. *Automation in Construction*, 2009. 18(5): p. 624-631.
- [9] Li, Y., P. Fazio, and J. Rao, An investigation of moisture buffering performance of wood paneling at room level and its buffering effect on a test room. *Building and Environment*, 2012. 47(1): p. 205-216.
- [10] Yoshino, H., T. Mitamura, and K. Hasegawa, Moisture buffering and effect of ventilation rate and volume rate of hygrothermal materials in a single room under steady state exterior conditions. *Building and Environment*, 2009. 44(7): p. 1418-1425.
- [11] Hameury, S., Moisture buffering capacity of heavy timber structures directly exposed to an indoor climate: a numerical study. *Building and Environment*, 2005. 40(10): p. 1400-1412.
- [12] Wang, W., R. Zmeureanu, and H. Rivard, Applying multi-objective genetic algorithms in green building design optimization. *Building and Environment*, 2005. 40(11): p. 1512-1525.
- [13] Calvino, F., et al., Comparing different control strategies for indoor thermal comfort aimed at the evaluation of the energy cost of quality of building. *Applied Thermal Engineering*, 2010. 30(16): p. 2386-2395.
- [14] Evins, R., et al., A case study exploring regulated energy use in domestic buildings using design-of-experiments and multi-objective optimisation. *Building and Environment*, 2012. 54(0): p. 126-136.
- [15] Li, K., et al., Optimization of ventilation system operation in office environment using POD model reduction and genetic algorithm. *Energy and Buildings*, 2013. 67(0): p. 34-43.
- [16] Smolka, J., Genetic algorithm shape optimisation of a natural air circulation heating oven based on an experimentally validated 3-D CFD model. *International Journal of Thermal Sciences*, 2013. 71(0): p. 128-139.
- [17] Lee, J.H., Optimization of indoor climate conditioning with passive and active methods using GA and CFD. *Building and Environment*, 2007. 42(9): p. 3333-3340.
- [18] Winkelmann, F.C., et al., DOE-2 Supplement Version 2.1E. 1993, Lawrence Berkeley National Laboratory: Springfield, VA
- [19] BSL, BLAST 3.0 Users Manual. 1999, Building Systems Laboratory, University of Illinois: Urbana-Champaign, IL.
- [20] Crawley, D.B., et al., EnergyPlus: creating a new-generation building energy simulation program. *Energy and Buildings*, 2001. 33(4): p. 319-331.
- [21] DOE, EnergyPlus Engineering Reference Version 8.0. 2013, Department of Energy: Washington, D.C.
- [22] Duffy, M.J., et al., TRNSYS: features and functionality for building simulation, in *Eleventh International IBPSA Conference 2009 Glasgow, Scotland*
- [23] Yan, D., et al., DeST — An integrated building simulation toolkit Part I: Fundamentals. *Building Simulation*, 2008. 1(2): p. 95-110.
- [24] Henninger, R.H. and M.J. Witte, EnergyPlus Testing with Building Thermal Envelope and Fabric Load Tests from ANSI/ASHRAE Standard 140-2011 2013, University of Central Florida: Arlington Heights, IL.
- [25] Hong, T., et al., Commercial building energy saver: an energy retrofit analysis toolkit. *Applied Energy*, 2015(159): p. 298-309.

- [26] Zhang, R., et al., A Novel Variable Refrigerant Flow (VRF) Heat Recovery System Model: Development and Validation. *Energy and Buildings*, 2018(168): p. 399–412.
- [27] Zhang, L., et al., Impact of post-rainfall evaporation from porous roof tiles on building cooling load in subtropical China. *Applied Thermal Engineering*, 2018(142): p. 391–400.
- [28] Zhang, R. and T. Hong, Modeling of HVAC operational faults in building performance simulation. *Applied energy*, 2017(202): p. 178-188.
- [29] Hong, T., et al., Development and Validation of a New Variable Refrigerant Flow Model in EnergyPlus. *Energy and Buildings*, 2016(117).
- [30] Sun, K., et al., A pattern-based automated approach to building energy model calibration. *Applied Energy*, 2016. 165: p. 214-224.
- [31] Tianzhen Hong, K.S., etc, Development and validation of a new variable refrigerant flow system model in EnergyPlus. *Energy and Buildings*, 2016. 117: p. 399-411.
- [32] Wetter, M., GenOpt: Generic Optimization Program User Manual. 2011, Lawrence Berkeley National Laboratory: Berkeley, CA
- [33] Karaguzel, O.T., R. Zhang, and K.P. Lam, Integrated Simulation Based Design Optimization of Office Building Envelopes for the Minimization of Life Cycle Costs, in *Proceedings of the Second International Conference on Building Energy and Environment (COBEE 2012)*. 2012: Boulder, USA.
- [34] MathWorks, MATLAB Tutorial. 2013, The MathWorks, Inc.: Natick, MA.
- [35] Bernal, W., et al., MLE+: a tool for integrated design and deployment of energy efficient building controls, in *Proceedings of the Fourth ACM Workshop on Embedded Sensing Systems for Energy-Efficiency in Buildings*. 2012, ACM: Toronto, Ontario, Canada. p. 123-130.
- [36] LBNL, ENERGYPLUS™ Energy Management System User Guide. 2012, Lawrence Berkeley National Laboratory: Berkeley, CA.
- [37] Karaguzel, O.T., R. Zhang, and K.P. Lam, Coupling of whole-building energy simulation and multi-dimensional numerical optimization for minimizing the life cycle costs of office buildings. *Building Simulation*, 2014. 7(2): p. 111-121.
- [38] Spitler, J.D., D.E. Fisher, and C.O. Pedersen. Radiant time series cooling load calculation procedure. in *Proceedings of the 1997 ASHRAE Annual Meeting*, June 28, 1997 - July 2, 1997. 1997. Boston, MA, USA: ASHRAE.
- [39] Spitler, J.D. and D.E. Fisher. On the relationship between the Radiant Time Series and Transfer Function Methods for design cooling load calculations. in *2000 ASHRAE Winter Meeting*, Feb 5 - Feb 9 2000. 2000. Dallas, TX, United states: Amer. Soc. Heating, Ref. Air-Conditioning Eng. Inc.
- [40] ASHRAE, Nonresidential cooling and heating load calculations, in *ASHRAE Handbook Fundamentals Chapter 30*. 2005, American Society of Heating, Refrigerating and Air-conditioning Engineers Inc.: Atlanta, GA.
- [41] Spitler, J.D. and B.A. Nigusse. Refinements and improvements to the radiant time series method. in *2010 ASHRAE Winter Conference*, January 23, 2010 - January 27, 2010. 2010. Orlando, FL, United states: Amer. Soc. Heating, Ref. Air-Conditioning Eng. Inc.
- [42] El Diasty, R., P. Fazio, and I. Budaiwi, Modelling of indoor air humidity: the dynamic behaviour within an enclosure. *Energy and Buildings*, 1992. 19(1): p. 61-73.
- [43] Harriman, L.G., D. Plager, and D. Kosar, Dehumidification and cooling loads from ventilation air. *Energy engineering*, 1999. 96(6): p. 31-45.
- [44] Mendes, N., et al., Moisture effects on conduction loads. *Energy and Buildings*, 2003. 35(7): p. 631-644.
- [45] Tariku, F., K. Kumaran, and P. Fazio, Determination of indoor humidity profile using a whole-building hygrothermal model. *Building Simulation*, 2011. 4(3): p. 277-277.
- [46] Deru, M., B. Griffith, and P. Torcellini, Establishing Benchmarks for DOE Commercial Building R&D and Program Evaluation. 2006, National Renewable Energy Laboratory: California.
- [47] ASHRAE, Energy Standard for Buildings Except Low-Rise Residential Buildings, in *ANSI/ASHRAE/IES Standard 90.1*. 2010, American Society of Heating, Refrigeration and Air-Conditioning Engineers, Inc: Atlanta.
- [48] Thornton, B.A., et al., Energy and Cost savings of ASHRAE Standard 90.1-2010. 2011, PNNL: Richland, WA.
- [49] Künzle, H.M., et al., Simulation of indoor temperature and humidity conditions including hygrothermal interactions with the building envelope. *Solar Energy*, 2005. 78(4): p. 554-561.
- [50] MathWorks, Optimization Toolbox™ User's Guide 2013, The MathWorks, Inc.: Natick, MA.
- [51] Lund, B.F. and B.A. Foss, Parameter ranking by orthogonalization—Applied to nonlinear mechanistic models. *Automatica*, 2008. 44(1): p. 278-281.

[52] Lin, W., Modeling and Optimization of a Semi-Interpenetrating Polymer Network Process. 2011, Carnegie Mellon University: Pittsburgh, Pennsylvania, USA.

[53] Yao, K.Z., et al., Modeling Ethylene/Butene Copolymerization with Multi-site Catalysts: Parameter Estimability and Experimental Design. *Polymer Reaction Engineering*, 2003. 11(3): p. 563-588.